Scripta Materialia 155 (2018) 11–15

Contents lists available at ScienceDirect

Scripta Materialia

journal homepage: www.elsevier.com/locate/scriptamat

Regular article

Large strain of lead-free bismuth ferrite ternary ceramics at elevated temperature

Ting Zheng [a], Chunlin Zhao [a], Jiagang Wu [a,*], Ke Wang [b], Jing-Feng Li [b]

[a] Department of Materials Science, Sichuan University, Chengdu 610064, PR China
[b] State Key Laboratory of New Ceramics and Fine Processing, School of Materials Science and Engineering, Tsinghua University, 100084 Beijing, PR China

ARTICLE INFO

Article history:
Received 9 February 2018
Received in revised form 30 April 2018
Accepted 2 June 2018
Available online xxxx

Keywords:
$BiFeO_3$-$BaTiO_3$
Ternary system
Strain property
Temperature dependence

ABSTRACT

Here we observed a large strain of lead-free $BiFeO_3$ ternary ceramics by the composition design [(0.70-x) $Bi_{1.05}FeO_3$-0.30$BaTiO_3$-xBi$(Mg_{2/3}Nb_{1/3})O_3$]. Positive temperature dependence of strain under $E = 4$ kV/mm can be observed in the ceramics with $x = 0.07$. Large strain property ($S = 0.32\%$ and $d_{33}^* = 800$ pm/V) and low hysteresis ($H = 5\%$) can be achieved in the ceramics measured at 200 °C, which may originate from thermally activated domain switching, electric field-induced relaxor to ferroelectric phase transition, and intrinsic lattice strain. We believe that the lead-free bismuth ferrite ternary ceramics with both large strain properties and small hysteresis are promising for high-temperature actuator applications.

The research interests in lead-free piezoelectric materials are greatly stimulated due to environmental concerns [1–3], and some exciting results about piezoelectric and strain properties were reported [4–11]. For example, the weak-field piezoelectric coefficient (d_{33}) of 570 pC/N and 620 pC/N was respectively obtained in lead-free $0.95K_{0.6}Na_{0.4}Nb_{0.965}Sb_{0.035}O_3$-$0.02BaZrO_3$-$0.03Bi_{0.5}K_{0.5}HfO_3$ and $Ba(Ti_{0.8}Zr_{0.2})O_3$-$(Ba_{0.7}Ca_{0.3})TiO_3$ ceramics by forming R-T phase boundary at room temperature [4–5]. Giant unipolar strain (0.7%) was achieved in $((Bi_{1/2}(Na_{0.84}K_{0.16})_{1/2})_{0.96}Sr_{0.04})(Ti_{0.975}Nb_{0.025})O_3$ (BNKT-2.5Nb) ceramics [6]. Although excellent piezoelectric properties of these materials can be obtained at room temperature, the deteriorated electrical properties at high temperatures greatly prohibit their practical applications [7–9]. Besides, ultrahigh external electric field and large hysteresis in BNT-based ceramics are tough issues for actuator applications [6]. Consequently, it is urgent to find another lead-free candidate with large strain and small hysteresis to meet the actuator applications.

Among the lead-free families, bismuth ferrite ($BiFeO_3$, BFO) has attracted lots of attentions due to high Curie temperature [12–14]. And relatively good performance at high temperatures makes it a promising candidate for high-temperature application [15–16]. However, strain behavior of BFO-based ceramics is often overlooked or underestimated. In addition, the enhanced strain usually requires the application of ultrahigh electric fields (E_{max}) [12, 17–19]. For example, large bipolar strain of ~0.36% (peak to peak value) was reported in pure BFO ceramic [17], and higher electric field ($E_{max} = 180$ kV/cm) was applied to trigger strain response in Sm-modified BFO ceramics [18]. A strain value (~0.37%) together with large hysteresis of ~39% was still induced in BFO-BTO-$BaZrO_3$ ceramics by applying high electric field (~70 kV/cm) [19]. Electrical properties of BFO-based ceramics are shown in Table 1. However, strain behavior was few studied by the use of small electric field. Therefore, it is highly expected to achieve large strain and small hysteresis in BFO-based ceramics under a small electric field (4 kV/mm) by composition modification, and then the physical mechanisms are discussed.

Here, we design the ternary ceramics of (0.70-x)$Bi_{1.05}FeO_3$-0.30$BaTiO_3$-xBi$(Mg_{2/3}Nb_{1/3})O_3$ (BFO-BTO-BMN). All ceramics were fabricated by the conventional solid-state method. Detailed preparation process and measurement condition are shown elsewhere [20]. Piezoelectric force microscopy (PFM) is carried out using a commercial microscope (MFP-3D, Asylum Research, Goleta, CA), applied to a conductive Pt-Ir coated cantilever PPP-NCHPt (Nanosensors, Switzerland).

Fig. 1(a) shows the XRD patterns of the ceramics with different x contents. All ceramics have a perovskite structure. The magnified XRD patterns ($2\theta = 31$–$32°$) are also presented in Fig. 1(a). A doublet peak changes to a singlet peak with increasing x, indicating the involvement of cubic-like phase. Previously, different phase boundaries were reported in the BFO-BTO systems, including rhombohedral-tetragonal (R-T) [21], rhombohedral-cubic (R-C) [22], rhombohedral-monoclinic (R-M) [23], and rhombohedral-pseudocubic (R-P_C) [24]. To characterize the phase structure of this work, Maud software is used to perform a full-pattern fitting for the ceramics with $x = 0.07$. Although singlet

* Corresponding author.
E-mail address: msewujg@scu.edu.cn (J. Wu).

https://doi.org/10.1016/j.scriptamat.2018.06.007
1359-6462/

Table 1
Strain properties of BFO-based ceramics.

Material system	Bipolar strain (%)	Unipolar strain (%)	d_{33}^* (pm/V)	Hysteresis (*H*)	E_{max} (kV/cm)	Ref
$BiFeO_3$(@RT)	$S_{pp} = 0.36$				150	[17]
$Bi_{0.88}Sm_{0.12}FeO_3$(@RT)	$S_{pp} = 0.30$				180	[18]
$Bi_{0.88}Sm_{0.12}Fe_{0.99}Ti_{0.01}O_3$(@RT)		0.07	46		150	[12]
0.75BF-0.25BZT(@RT)		0.265	265	30	100	[29]
0.63BF-0.33BT-0.04$BaZrO_3$(@RT)		0.37	528	39	70	[19]
$Bi_{0.98}Nd_{0.02}FeO_3$-BT(@150 °C)		0.43	716	18	60	[16]
0.7BF-0.3BT-MnO_2(@180 °C)		0.26	652	25	40	[30]
BF-BT-(Bi,Mg)NbO_3(@200 °C)		0.32	800	5	40	This work

peaks appear in the sample, poor fitting results (Sig > 2.0) are obtained based on single phase mode, such as R, T, C, and M (Not shown here). Therefore, single phase can be eliminated. Fig. 1(b–d) shows the full-pattern fitting based on R3m-Pm3m, R3m-P4mm, and R3m-C1m1 modes, respectively. Compared with the case of R-M, much better matching results between the observed and calculated patterns can be observed in the case of R-C and R-T [Fig. 1(b–c)]. The goodness-of-fit indicators Sig and another factor Rwp are 1.38, 1.61 and 4.94, 5.79 respectively [Table 2]. All these results indicate that the Rietveld refinement based on R-C is more reliable. Relatively good refinement based on R-T can be attributed to the similar lattice parameters between highly symmetric C and T phases [Table 2]. Therefore, it can be suggested that both R and pseudo cubic phases should exist here. However, the exact phase symmetry of pseudo cubic (T or C) is still difficult to identify, which needs further advanced exploration. The temperature-dependent dielectric constant (ε_r-*T*) of the ceramics with $x = 0.01$ and $x = 0.07$ are shown in Fig. 1(e). The ceramics with $x = 0.07$ exhibit frequency dispersion and diffuse phase transition behavior at T_m. The modified Curie-Weiss law $1/\varepsilon_r - 1/\varepsilon_m = (T-T_m)^\gamma/C$ has been applied to analyze the diffuse phase transition, and the Ln($1/\varepsilon_r$-$1/\varepsilon_m$) *versus* Ln(T-T_m) curves of the ceramics with $x = 0.01$ and $x = 0.07$ are plotted in Fig. 1(f) to calculate the diffuseness degree γ. The γ and another parameter

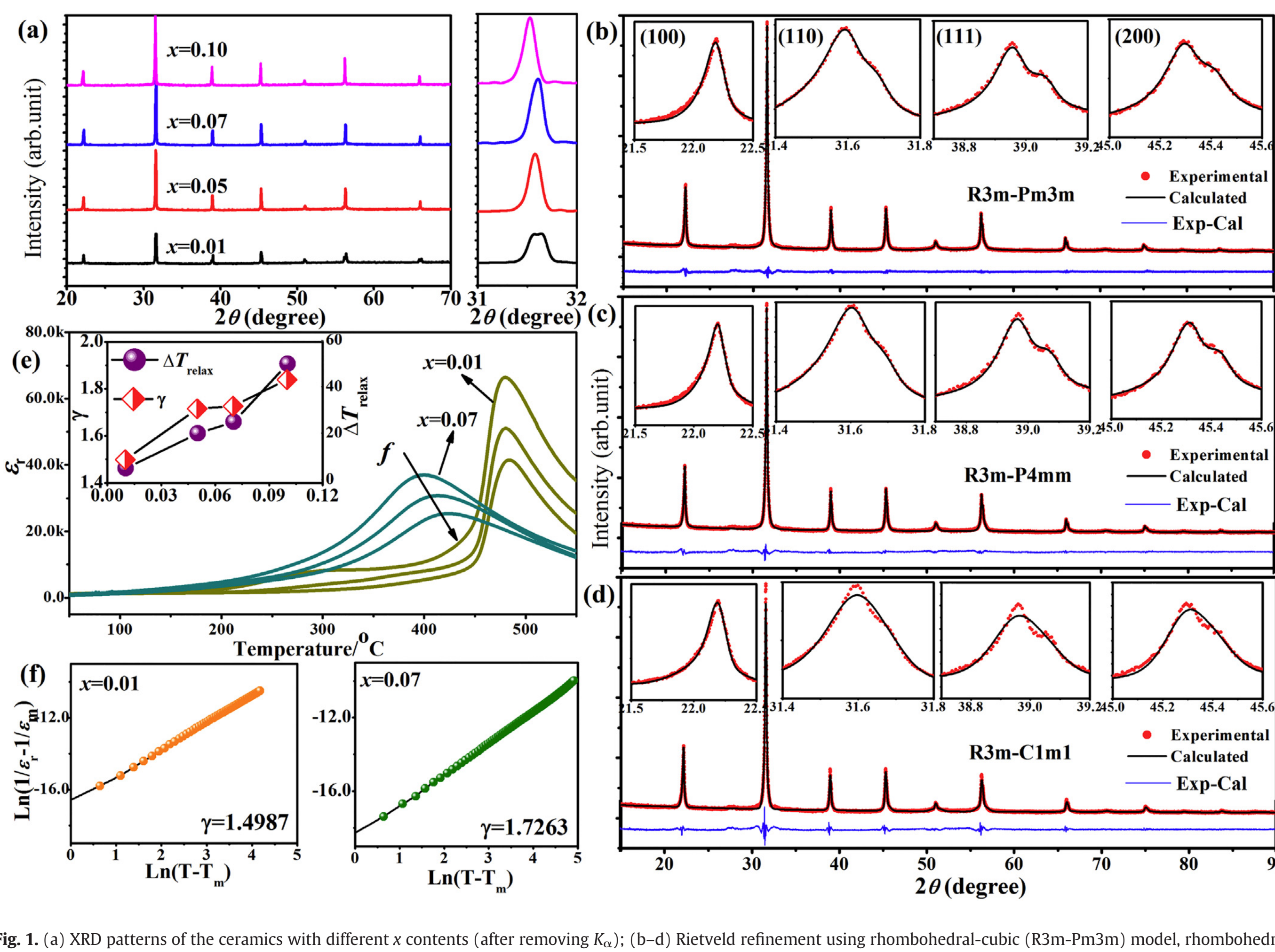

Fig. 1. (a) XRD patterns of the ceramics with different *x* contents (after removing K_α); (b–d) Rietveld refinement using rhombohedral-cubic (R3m-Pm3m) model, rhombohedral-tetragonal (R3m-*P*4mm) model, and rhombohedral-monoclinic (R3m-C1m1) mode; (e) temperature dependence of dielectric constant and (f) Ln($1/\varepsilon_r$-$1/\varepsilon_m$) *versus* Ln(*T*-T_m) of $x = 0.01$ and $x = 0.07$; Inset of Fig. 1(e) is the diffuseness degree γ and ΔT_{relax} as a function of *x* content.